Provided for non-commercial research and education use.
Not for reproduction, distribution or commercial use.

This article appeared in a journal published by Elsevier. The attached copy is furnished to the author for internal non-commercial research and education use, including for instruction at the authors institution and sharing with colleagues.

Other uses, including reproduction and distribution, or selling or licensing copies, or posting to personal, institutional or third party websites are prohibited.

In most cases authors are permitted to post their version of the article (e.g. in Word or Tex form) to their personal website or institutional repository. Authors requiring further information regarding Elsevier's archiving and manuscript policies are encouraged to visit:

http://www.elsevier.com/authorsrights

Author's personal copy

Thin Solid Films 557 (2014) 70–75

Contents lists available at ScienceDirect

Thin Solid Films

journal homepage: www.elsevier.com/locate/tsf

Molecular-beam epitaxial growth of tensile-strained and *n*-doped Ge/Si(001) films using a GaP decomposition source

T.K.P. Luong [a], A. Ghrib [b], M.T. Dau [a], M.A. Zrir [a], M. Stoffel [c], V. Le Thanh [a], R. Daineche [d], T.G. Le [a], V. Heresanu [a], O. Abbes [a], M. Petit [a], M. El Kurdi [b], P. Boucaud [b], H. Rinnert [c], J. Murota [e]

[a] Aix-Marseille Université, CNRS CINaM-UMR 7325, F-13288 Marseille Cedex 09, France
[b] Institut d'Electronique Fondamentale, CNRS UMR 8622, Université Paris-Sud, Bât. 220, F-91405 Orsay, France
[c] Université de Lorraine, Institut Jean Lamour, UMR CNRS 7198, Nancy-Université, BP 70239, F-54506 Vandoeuvre-lès-Nancy Cedex, France
[d] Aix-Marseille Université, CNRS IM2NP-UMR 6242, F-13397 Marseille Cedex 20, France
[e] Res. Inst. Elec. Comm., Tohoku University, 2-1-1 Katahira, Aoba-ku, Sendai 980-8577, Japan

ARTICLE INFO

Available online 20 November 2013

Keywords:
Tensile strain Ge
n-Doping
MBE growth
Optoelectronics

ABSTRACT

We have combined numerous characterization techniques to investigate the growth of tensile-strained and *n*-doped Ge films on Si(001) substrates by means of solid-source molecular-beam epitaxy. The Ge growth was carried out using a two-step growth method: a low-temperature growth to produce strain relaxed and smooth buffer layers, followed by a high-temperature growth to get high crystalline quality Ge layers. It is shown that the Ge/Si Stranski–Krastanov growth mode can be completely suppressed when the growth is performed at substrate temperatures ranging between 260 °C and 300 °C. X-ray diffraction measurements indicate that the Ge films grown at temperatures of 700–770 °C are tensile-strained with typical values lying in the range of 0.22–0.24%. Cyclic annealing allows further increase in the tensile strain up to 0.30%, which represents the highest value ever reported in the Ge/Si system. *n*-Doping of Ge was carried out using a GaP decomposition source. It is shown that heavy *n*-doping levels are obtained at low substrate temperatures (210–250 °C). For a GaP source temperature of 725 °C and a substrate temperature of 210 °C, a phosphorus concentration of about 10^{19} cm^{-3} can be obtained. Photoluminescence measurements reveal an intensity enhancement of about 16 times of the direct band gap emission and display a redshift of 25 meV that can be attributed to band gap narrowing due to a high *n*-doping level. Finally, we discuss about growth strategies allowing optimizing the Ge growth/doping process for optoelectronic applications.

© 2013 Elsevier B.V. All rights reserved.

1. Introduction

In recent years, research on tensile-strained and *n*-doped Ge epilayers has been the subject of numerous investigations [1–13], work in this direction being driven by the hope to use Ge as an active layer in optoelectronic devices. Indeed, it has been shown that when a tensile strain is applied to Ge, the energy position of the conduction Γ valley decreases faster than the one of the band-edge L valley [14] and a transition from indirect to direct band gap can occur for an in-plane tensile strain of ~1.9% [15]. On the other hand, *n*-type doping of Ge leads to a more efficient population of the zone center Γ valley and thus enhances optical recombination at the Brillouin zone center [16,17].

In the Ge/Si system, tensile strain can be thermally generated from the difference in the thermal expansion coefficients between Ge and Si. There are in fact two kinds of strain that can be induced in a Ge film when growing on Si: compressive strain and tensile strain. In the early growth stage, since the Ge lattice parameter is 4.2% larger than that of Si, the Ge film will be laterally compressed to accommodate its in-plane lattice parameter to that of Si. Such a growth regime, called pseudomorphic, can be maintained up to the so-called critical thickness, beyond which strain relaxation takes place. It is now well recognized that the strain relaxation proceeds via two steps when increasing the film thickness: the first is a partial elastic strain relaxation, which is often accompanied by a growth mode transition from two-dimensional (2D) growth to islanding (3D) growth [18]; the second is a plastic relaxation process along which both misfit and threading dislocations are generated. Tensile strain can be induced in Ge when growing at high temperatures and subsequent cooling down because Ge has a thermal expansion coefficient twice larger than that of Si. Thus, when a Ge film with a thickness higher than the critical thickness of a few nanometers (nm) is deposited on a Si substrate at a temperature higher than 400 °C and then is cooled down to room temperature, the Ge film is tensile-strained but exhibits a high density of threading and misfit dislocations. At the same time, the film surface becomes very rough due to a transition from 2D to 3D growth. In general, the surface roughness and the density of threading dislocations depend on the film thickness, the substrate temperature and also on the growth technique. For a film of a few hundreds nm thick that is grown at a substrate

E-mail address: lethanh@cinam.univ.mrs.fr (V. Le Thanh).

0040-6090/$ – see front matter © 2013 Elsevier B.V. All rights reserved.
http://dx.doi.org/10.1016/j.tsf.2013.11.027

Author's personal copy

temperature lying in the range of 600–700 °C, the density of threading dislocations can reach a value as high as 10^7–10^8 cm^{-2}. To improve the crystalline quality of Ge films, a two-step growth method has been proposed [19,20], which consists of a low-temperature growth to form strain relaxed and smooth buffer layers, followed by a growth at higher temperatures to produce thicker films of high crystalline quality. However, up to now most of the above-mentioned investigations have been mainly carried out using chemical vapor deposition (CVD) and only a few of them have concerned molecular-beam epitaxial (MBE) growth [5–7]. It is now recognized that the low-temperature growth step is crucial to control the final state of the film crystalline quality. The degree of freedom regarding the choice of the substrate temperature is rather limited within the CVD technique. Indeed, in a standard CVD process, the thermal energy should be high enough to dissociate the gas precursor molecules. For this reason, in previous works the low-temperature step has been indeed carried out at an intermediate temperature often higher than 350 °C [1–4,12,13]. As a consequence of this temperature, Ge films grown by CVD display a high density of stacking faults and defects [12,13,21].

In this work, we report results of the growth and *n*-doping of Ge/Si(001) films using solid-source MBE. We have focused on the control of both the crystalline quality and the surface roughness during the low-temperature growth step. The Ge growth was investigated within a wide temperature range, going from room temperature to 550 °C. We have evidenced the existence of a narrow substrate temperature window, from 260 to 300 °C, in which the Stranski–Krastanov growth of Ge on Si can be completely suppressed. The resulting Ge epilayers are shown to be almost free of threading dislocations and display a relatively smooth surface. Concerning *n*-type doping of Ge, since tetrahedral white phosphorus (P_4 molecules) is not stable and highly volatile, we have used a specific doping cell based on the decomposition of GaP to produce diphosphorus (P_2 molecules). It is shown that a phosphorus doping level higher than 10^{19} cm^{-3} can be obtained.

2. Experimental details

Ge growth was performed in a standard MBE system with a base pressure better than 5×10^{-8} Pa. The growth chamber is equipped with a 30-keV reflection high-energy electron diffraction (RHEED) apparatus, which allows us to monitor in *real time* the Ge growth mode. An Auger electron spectrometer is used to control the cleanliness of the substrate surface prior to growth and the efficiency of Ga trapping of the GaP source. Ge was evaporated from a two-zone heated Knudsen effusion cell and the Ge deposition rate, measured using RHEED intensity oscillations during Ge homoepitaxy on a Ge(111) substrate, was in the range between 1.5 and 5 nm/min.

The substrates were flat, *p*-type Si(001) wafers. Cleaning of the substrate surface followed the hydrogen-terminated Si(001) method, which consists of two steps: the first was a wet chemical treatment in NH_4F solution to prepare an ideally SiH_2-terminated Si(001) surface [22]. The second step is heating in ultrahigh vacuum to desorb the passivating hydrogen layer at a temperature of about 500 °C. After this step, the Si surface exhibits a well-developed (2 × 1) reconstruction and AES measurements do not reveal any presence of oxygen or carbon. The substrate temperature was measured using a thermocouple in contact with the backside of the Si wafers. The accuracy of the temperature measurement is estimated to be about ± 20 °C.

The structural properties of the as-grown films were investigated by means of high-resolution transmission electron microscopy (HRTEM) using a JEOL 3010 microscope operating at 300 kV with a spatial resolution of 0.17 nm. The strain level in the Ge epilayer was deduced from X-ray diffraction (XRD) measurements performed using a diffractometer (Philips X'pert MPD) equipped with a copper target for Cu-$K_{\alpha 1}$ radiation ($\lambda = 1.54059$ Å). The angular resolution is ~0.01°. To quantify the density of threading dislocations in Ge films, we used selective defect-etching in a chromium-based chemical solution for the revelation of threading dislocations. The density of threading dislocations was measured by a JEOL Scanning Electron Microscope.

The phosphorus concentration profiles in doped samples were measured by secondary ion mass spectrometry (SIMS), using Cs^+ primary ion beams at 1 kV impact energy and with an incidence angle of about 68.4° from the normal of the sample surface. The phosphorus profiles were calibrated using P ion implanted Ge samples with various P concentrations; the depth calibration was performed using crater Alpha-step depth measurement. The detection limit of our SIMS measurements is below 10^{14} $a \cdot cm^{-3}$.

The photoluminescence is measured with a 532 nm laser focused on the sample surface; the incident power density is typically in the tens of kW cm^{-2}. The photoluminescence signal is measured with a PbS detector, thus, allowing covering a large spectral range without detector cutoff. Photoluminescence spectra were recorded at room temperature.

3. Results and discussion

As compared to material growth in a CVD reactor, the MBE growth chamber is equipped with RHEED, which is a powerful technique allowing us to monitor in *real-time* the change of both the surface morphology and the surface structure of the growing film. By means of RHEED, we have investigated the Ge growth in a large temperature range, from room temperature to 550 °C, and we have evidenced the existence of a narrow temperature window from 260 °C to 300 °C in which the Stranski–Krastanov Ge/Si growth can be completely suppressed [23]. In this temperature window, two-dimensional streaky RHEED patterns of the Ge growing surface are continuously observed from the first layer up to a film thickness of a few hundreds of nm. Fig. 1a shows a typical cross-sectional TEM image of a 300 nm thick Ge layer, which has been grown following the two-step growth method: 50 nm thick Ge layer deposited at 300 °C followed by a 250 nm thick Ge film grown at 730 °C. First, we emphasize that during Ge growth in the low- and high-temperature regimes, RHEED patterns remain two-dimensional, characteristic of a smooth surface. The image clearly reveals that misfit dislocations have not spread out as in the case of CVD growth [12,13,21] but are mainly confined near the Ge/Si interface. This can be better seen in a HRTEM image taken near the interface region (Fig. 1b) in which an atomically resolved Ge/Si interface is observed. Some threading dislocations (indicated by white arrows) are visible but interestingly SEM measurements performed after defect etching using a Cr-based solution (not shown here) show that threading dislocations have gathered together to form defected regions having a circular or square shape. The size of these defected regions varies from sub-μm to larger than a hundred μm and if we assume that a defected region corresponds to a *threading dislocation unit*, we can obtain a density of threading dislocations below 10^4 cm^{-2} [23].

The high-temperature growth step has been investigated at various temperatures: 400, 500, 600, 650, 700, 750 and 770 °C. Fig. 2a displays some representative Ω–2θ XRD scans taken around the Ge(004) reflection. For comparison, we report in dotted green lines an XRD scan of a sample grown at 300 °C. The fact that the Ge(004) reflection of the sample grown at 300 °C is located at 2θ ~ 66°, a value close to that measured on a Ge substrate, indicates that the corresponding Ge layer is almost fully relaxed. When the growth temperature increases from 300 to 700 °C, the 2θ angle value of the Ge(004) reflection is found to monotonously increase and then remains almost constant for further increase of the growth temperature up to 770 °C. To determine the value of the in-plane tensile strain $\varepsilon_{//}$, we first deduce the out-of-plane strain ($\varepsilon_{\perp}$) from the θ–2θ XRD curves and then determine the value of $\varepsilon_{//}$ using the following relationship:

$$\varepsilon_{//}\left(\varepsilon_{//} + \varepsilon_{\perp}\right) = c_{11}/(c_{11} + 2c_{12})$$

Author's personal copy

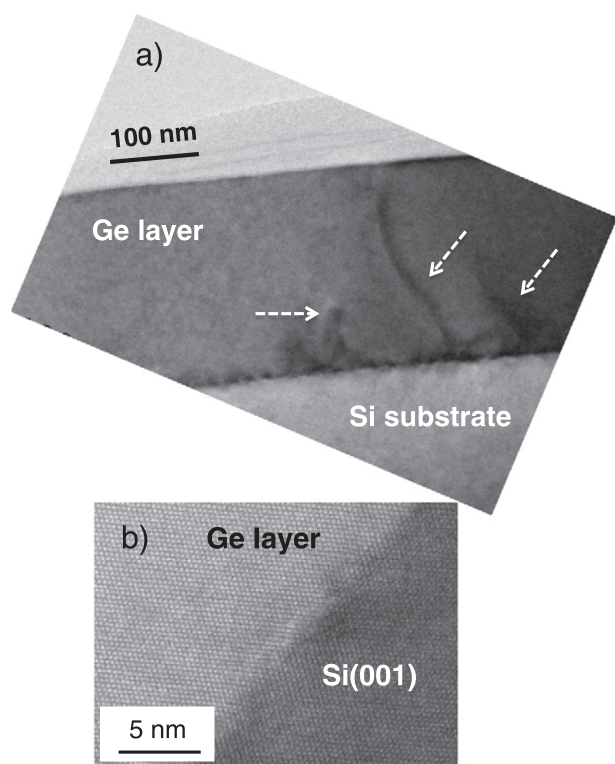

Fig. 1. a) Typical cross-sectional TEM image of a ~300 nm thick Ge layer grown on Si(001) following the two-step growth at 300/730 °C. White arrows indicate some threading dislocations that may be generated during the increase of the substrate temperature to the high-temperature growth step; b) A zoom taken near the interface region, illustrating the flatness at the atomic scale of the interface.

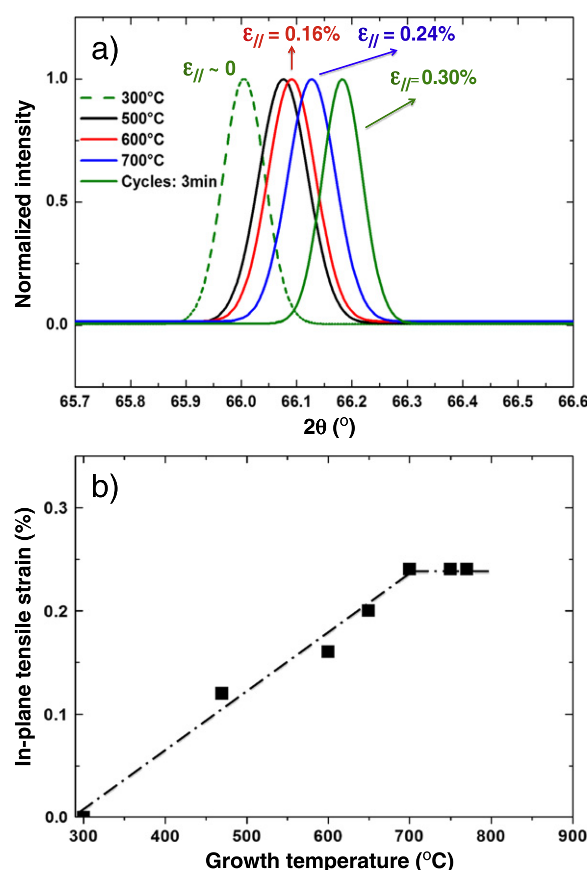

Fig. 2. a) Evolution of θ–2θ XRD scans around the Ge(004) reflection with the growth temperature and cyclic annealing. The dotted XRD scan corresponding to a sample grown at 300 °C is shown for comparison. The solid green curve corresponds to 10 annealing cycles from 780 to 900 °C with an annealing time of 3 min at each temperature; b) Evolution of the tensile strain versus growth temperature.

with elastic constants $c_{11} = 12.85 \times 10^{10}$ Pa and $c_{12} = 4.83 \times 10^{10}$ Pa for pure Ge [24]. The highest value of the in-plane tensile strain $\varepsilon_{//}$ obtained in the growth temperature range of 700–770 °C is 0.24%, which is in good agreement with previous results reported using CVD in which the highest tensile strain was in the range of 0.22–0.25% at similar growth temperatures [1–3,12,13]. This confirms that a value of the tensile strain of about 0.25% probably represents the highest value that can be obtained by using the high-temperature growth step. Shown in Fig. 2b is a summary of the evolution of the in-plane tensile strain versus growth temperature. It is worth noting that for a Ge growth at a temperature higher than 800 °C, long-range Ge/Si interdiffusion occurs, which can deteriorate both the optical and transport properties of the Ge layer.

To understand the above evolution of the tensile strain, in particular the saturation of the tensile strain when the growth temperature is higher than 700 °C, we recall that as the tensile strain in the Ge epilayer arises from the difference of thermal expansion coefficients between Ge and Si, it may expect that the tensile strain continuously increases when increasing the growth temperature beyond 700 °C. However, as the Ge lattice parameter is 4.2% larger than that of Si, the Ge epilayer is linked to the Si substrate via a high density of misfit dislocations that are located near the interface region. The presence of such interface dislocations may prevent the Ge epilayer to be freely distorted at high growth temperatures, thus limiting the value of the tensile strain in the Ge epilayer.

After growth, the samples were subjected to the thermal annealings not only to reduce the density of threading dislocations but also to increase the tensile strain. Indeed, once the Ge epilayer has a certain tensile strain, upon annealing it will not behave as a perfect elastic material in which the stress–strain characteristic is ideally linear and the strain variation curve is perfectly superimposed over the stress variation curve. The Ge epilayer will behave visco-elastically and nonlinear behavior of stress–strain curve appears. Two methods of thermal annealing have been used, a long anneal at 900 °C and cyclic annealings from 780 to 900 °C. It has been found that cyclic annealings are more efficient regarding the introduction of additional strain in the Ge films. The XRD curve measured after ten annealing cycles from 780 to 900 °C with an annealing time of 3 min at each temperature is shown in Fig. 2 (green solid curve). The as-grown sample was deposited at 600 °C and its corresponding in-plane tensile strain is 0.16%. As can be seen, after cyclic annealings, the tensile strain in the layer has increased up to 0.30%. The above result indicates that an adequate combination of the two-step growth method, in particular the control of the low-temperature growth step, with cyclic annealing allows getting Ge epilayers having a high crystalline quality, a smooth surface and also a high level of tensile strain. It is worth noting that the tensile-strain determination from asymmetric (224) and (−2–24) is in good agreement with the above value deduced from the symmetric (004) reflection. In addition, we have also proceeded cyclic annealings for samples grown at 650 and 700 °C and a similar value of tensile strain was obtained. These results clearly confirm the effectiveness of the cyclic annealings to further increase the tensile strain in the Ge epilayers. However, we have found out that the increase in the tensile strain and Ge/Si interdiffusion are competing processes, so that for a sample that has been grown at a high temperature, for example at 700 °C, the number of annealing cycles and the annealing time should be optimized to control the degree of Ge/Si interdiffusion.

The above maximum strain value is, however, significantly lower than that required for the transition from an indirect to a direct band gap Ge (i.e. ~1.9%). To achieve direct band gap conditions, alternative

Author's personal copy

strategies such as *n*-doping have to be explored. To evaluate the efficiency of *n*-doping from the decomposition of GaP, one of the first parameters that needs to be controlled is the temperature range of the GaP cell in which only phosphorus can evaporate. Indeed, GaP is decomposed into Ga and P_2 and at an intermediate temperature range it is expected that only P_2 can escape from the cell while Ga will be trapped by a cap placed on top of the cell [25]. We have then grown a stacked structure, consisting of three P-doped Ge layers, which are separated by a 80 nm thick Ge spacer layer. A scheme of the stacked structure is shown in Fig. 3a. For the P-doped Ge layers, the temperature of the GaP cell was set at 600, 700 and 800 °C. The substrate temperature is chosen to be 300 °C since during Ge growth; it has been observed that the Ge growth is two-dimensional and threading dislocations are almost absent at this temperature. Thus, at 300 °C it is expected that the Ge layer will be uniformly doped with phosphorus. Fig. 3b displays SIMS measurements of the P concentration (blue curve) and Ge concentration (red curve) profiles across the stacked structure. Three values of the P concentration are obtained: 3×10^{17}, 6×10^{18} and $\sim 4 \times 10^{20}$ cm^{-3}, which correspond to three temperatures of the GaP cell of 600, 700 and 800 °C, respectively. Thus, SIMS measurements seem to indicate that phosphorus sublimation is the most efficient at a GaP source temperature of 800 °C. However, electrical measurements (not shown here) show that the lowest resistivity is obtained for a GaP source temperature of 725 °C. We thus expect that at temperatures higher than 725 °C, a tiny amount of Ga, whose concentration is below the SIMS detection limit, can escape from the cell, leading to a deterioration of the transport properties.

We have therefore kept the GaP source at a constant temperature of 725 °C and investigated the effect of the doping level versus the substrate temperature. Fig. 4a shows room-temperature current–voltage curves measured at various substrate temperatures. We note that all samples investigated here have a total thickness of 100 nm (30 nm thick undoped Ge layer deposited at 300 °C to form a smooth and strain relaxed buffer layer, followed by a 70 nm P-doped Ge film deposited at various substrate temperatures). It can be clearly seen that the resistivity decreases when decreasing the substrate temperature and the lowest resistivity is obtained at a temperature of 210 °C. The evolution of the resistivity versus substrate temperature is summarized in Fig. 4b. To explain this behavior, it is worth noting that the efficiency of phosphorus doping may depend on two main parameters: the solubility of phosphorus in the Ge lattice and the sticking coefficient of P_2 molecules on the Ge surface. For the first parameter, it has been shown in the case of Si that the phosphorus solubility increases with increasing the substrate temperature and the highest value of the solubility is obtained at a temperature above 1300 °C [26]. On the other hand, the sticking coefficient of a molecule on a substrate surface should increase with decreasing the substrate temperature. Since our results reveal that P doping is more favorable at low substrate temperatures, it appears that the sticking coefficient of P_2 is the dominant parameter determining the phosphorus doping level in Ge. We also note that the above behavior of P doping is similar to the case of Sb doping in Ge in which high doping levels were observed in the temperature range of 160–250 °C [27].

Fig. 5 shows the evolution of the photoluminescence spectrum with the substrate temperature, the temperature of the GaP source being fixed at 725 °C. The samples are similar to those used for the above electrical characterizations. The reference sample is a 100 nm thick undoped Ge layer deposited at a substrate temperature of 300 °C. The spectrum of the reference sample exhibits a very weak intensity and direct band gap emission is not clearly observed, as expected. The PL intensity, which is very weak for the sample deposited at 500 °C, is found to increase with decreasing the substrate temperature and the highest

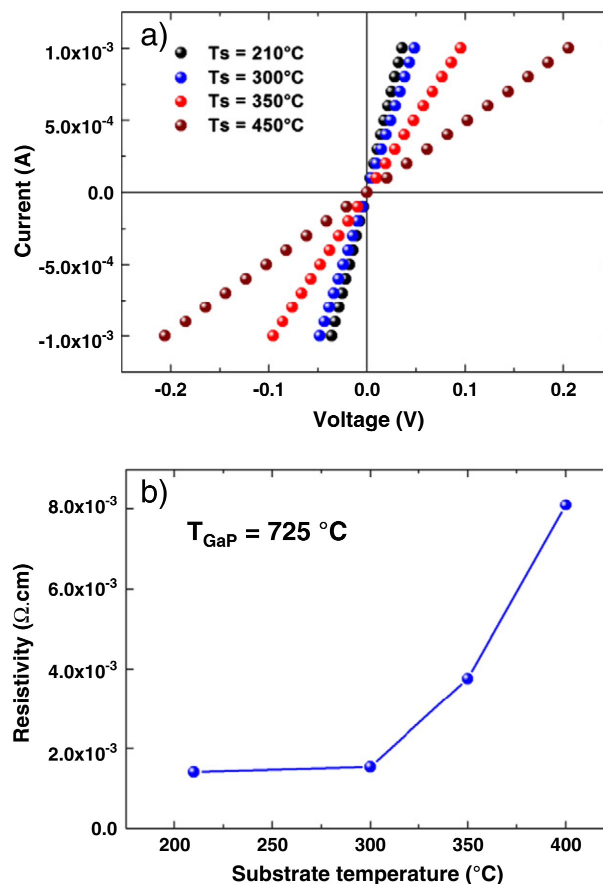

Fig. 4. a) Room-temperature current–voltage curves measured for samples grown at various substrate temperatures; b) Evolution of the layer resistivity versus substrate temperature. The temperature of the GaP cell is 725 °C.

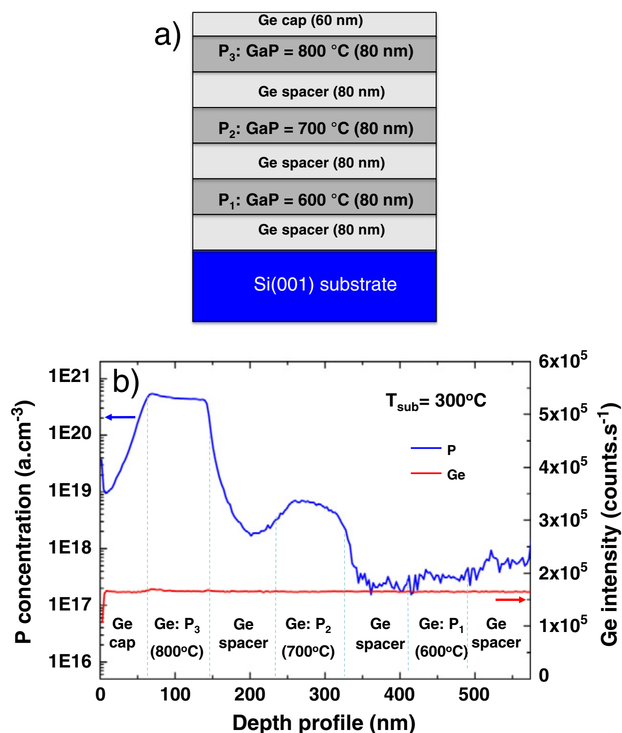

Fig. 3. a) Schema representing a stacked structure that has been used to determine the phosphorus concentration at different temperatures of the GaP cell. The substrate temperature is 300 °C; b) SIMS measurements of phosphorus (blue curve) and Ge (red curve) concentration profiles. The phosphorus concentrations of 3×10^{17}, 6×10^{18} and up to $\sim 4 \times 10^{20}$ cm^{-3} are obtained for the GaP cell temperatures of 600, 700 and 800 °C, respectively.

Author's personal copy

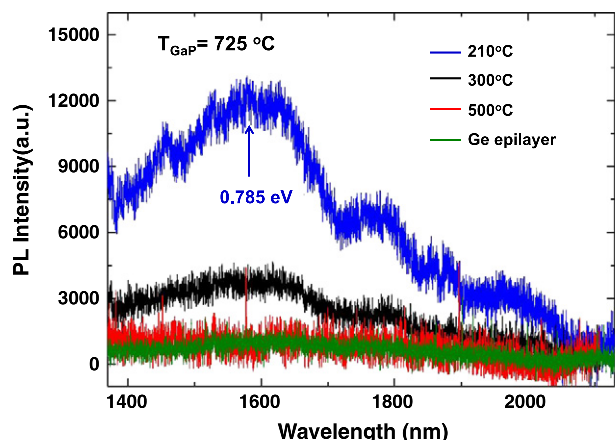

Fig. 5. Evolution of the photoluminescence spectrum versus the growth temperature. All photoluminescence spectra were recorded at room temperature.

PL intensity is obtained for a substrate temperature of 210 °C. We note that this evolution follows almost the same trend already observed for the electrical measurements (Fig. 4) and thus confirms the efficiency of P doping at low substrates temperatures. At 210 °C, the PL spectrum peaks at around 1580 nm (i.e. the corresponding energy is 0.785 eV). This transition can be attributed to arise from the direct band gap radiative recombinations in the *n*-doped Ge layer. As compared to the energy maximum around 0.810 eV, arising from the direct band gap emission of unstrained and undoped Ge, we observe here a redshift of 25 meV, which can be attributed to band gap narrowing at high *n*-doping levels. Indeed, as shown in Fig. 2, a low-temperature growth at 210 °C does not induce tensile strain in the Ge film and the optical redshift can thus directly be correlated to the effect of *n*-doping. It is worth noting that according to ref., a redshift of 25 meV corresponds to a doping level of ~2×10^{19} cm^{-3}, which is in agreement with our SIMS measurements. Indeed, in Fig. 3 SIMS measurements indicate a phosphorus concentration of 6×10^{18} cm^{-3} at a GaP cell temperature of 700 °C and other SIMS measurements at 725 °C (not shown here) provide a phosphorus concentration of about 10^{19} cm^{-3}. Another noteworthy point is that if we compare the photoluminescence intensity of the sample doped at 210 °C (blue curve) with that of the undoped sample (green curve), an optical enhancement of about 16 times is obtained. Finally, we note that multi-shoulders/cuttings, which are observed in the wavelength range of 1750–2000 nm of the PL spectrum of the sample doped at 210 °C, can be attributed to arise from humidity absorption in ambient air. In fact, due to a relatively weak photoluminescence intensity, the photoluminescence signal was collected with a low resolution spectrometer. When the spectrometer resolution is increased, multiple and separate absorption peaks appear in this wavelength range.

The separate investigation of the effect of the substrate temperature on the tensile strain and *n*-doping of the Ge layer brings fruitful information. The substrate temperature is shown to produce an opposite effect on these two properties of the Ge film. Higher growth temperatures (up to 770 °C) induce larger tensile strain while low temperatures favor *n*-doping. It is noteworthy that an *n*-doping level higher than 10^{19} cm^{-3} can be obtained at a growth temperature of 210 °C. However, it should be pointed out that at this substrate temperature, the Ge/Si growth does proceed via the Stranski–Krastanov mode but the corresponding 3D growth is, in some ways, much less pronounced as compared with the growth at temperatures higher than 300 °C. To adopt an adequate strategy to produce Ge epilayers for optoelectronic applications, first it is important to emphasize that the thermal-induced tensile train is limited to a value lying in the range of 0.25–0.30%, which is far from the expected value to get direct bandgap conditions for Ge. Thus, it would be preferable to set up growth conditions, which favor *n*-doping. In other words, heavy *n*-doping appears to be the parameter that is more important than the value of the tensile strain. This implies that an adequate strategy would be to grow and to *n*-dope Ge films at low temperatures followed by post-growth thermal annealing. However, Ge films grown and *n*-doped at low temperatures usually contain a high density of point defects (vacancies and interstitials). Therefore, thermal annealing should be optimized not only to restore the crystalline quality of the layer but also to activate dopants to occupy substitutional sites. Co-doping of P with other elements, such as As and Sb, can be also envisaged in order to overcome the solubility limit of an doping element in the Ge lattice.

4. Conclusion

In summary, we have separately investigated the effect of the substrate temperature on the tensile strain and *n*-doping of Ge films grown on Si(001) substrates using a two-step growth method by solid-source MBE. We have evidenced the existence of a narrow substrate temperature window from 260 to 300 °C in which it is possible to completely suppress the Ge/Si Stranski–Krastanov growth. The tensile strain is found to linearly increase with the growth temperature, reaching maximum values in the range of 0.22–0.24%. Similar values have been reported for CVD grown films. Post-growth annealing can further increase the tensile strain in Ge films up to 0.30%, which is one of the highest values ever reported for the Ge/Si system. We have also presented primary results of P-doping using the decomposition of GaP. It is found that high *n*-doping levels are obtained at low substrate temperatures (210–250 °C). Compared to the undoped sample, photoluminescence measurements of a highly doped sample reveal a photoluminescence enhancement of about 16 times and display a redshift around 25 meV due to band gap narrowing at a doping level of ~2×10^{19} cm^{-3}.

The substrate temperature is found to produce an opposite effect to the tensile strain and *n*-doping. Since thermal-induced tensile strain in the Ge/Si is limited to 0.25–0.30%, optimizing the growth condition to favor heavy *n*-doping in Ge plays an important role for the development of Ge-based optoelectronics. It appears that Ge growth and doping at a low temperature (200–250 °C) followed by thermal annealing would be an efficient approach.

Acknowledgments

This work was supported by the French ANR Program via the GRAAL project (Blanc 2011 BS03 004 01) and partially supported by the JSPS Core-to-Core Program, Advanced Research Networks “International Collaborative Research Center on Atomically Controlled Processing for Ultralarge Scale Integration”.

References

[1] J. Liu, X. Sun, D. Pan, X. Wang, L.C. Kimerling, T.L. Koch, J. Michel, Opt. Express 15 (2007) 11272.
[2] J. Liu, X. Sun, R. Camacho-Aguilera, L.C. Kimerling, J. Michel, Opt. Lett. 35 (2010) 679.
[3] J. Liu, R. Camacho-Aguilera, J.T. Bessette, X. Sun, X. Wang, Y. Cai, L.C. Kimerling, J. Michel, Thin Solid Films 520 (2012) 3354.
[4] Y. Ishikawa, K. Wada, Thin Solid Films 518 (2010) S83.
[5] E. Kasper, M. Oehme, J. Werner, T. Aguirov, M. Kittler, Front. Optoelectron. 5 (2012) 256.
[6] J. Werner, M. Oehme, M. Schmid, M. Kaschel, A. Schirmer, E. Kasper, J. Schulze, Appl. Phys. Lett. 98 (2011) 061108.
[7] M. Oehme, M. Gollhofer, D. Widmann, M. Schmid, M. Kaschel, E. Kasper, J. Schulze, Opt. Express 21 (2013) 2206.
[8] Y. Bai, K.E. Lee, C. Cheng, M.L. Lee, E.A. Fitzgerald, J. Appl. Phys. 104 (2008) 084518.
[9] M. El Kurdi, H. Bertin, E. Martincic, M. de Kersauson, G. Fishman, S. Sauvage, A. Bosseboeuf, P. Boucaud, Appl. Phys. Lett. 96 (2010) 041909.
[10] R. Jakomin, M. de Kersauson, M. El Kurdi, L. Largeau, O. Mauguin, G. Beaudoin, S. Sauvage, R. Ossikovski, G. Ndong, M. Chaigneau, I. Sagnes, P. Boucaud, Appl. Phys. Lett. 98 (2011) 091901.
[11] A. Ghrib, M. de Kersauson, M. El Kurdi, R. Jakomin, G. Beaudoin, S. Sauvage, G. Fishman, G. Ndong, M. Chaigneau, R. Ossikovski, I. Sagnes, P. Boucaud, Appl. Phys. Lett. 100 (2012) 201104.

Author's personal copy

[12] J.-M. Hartmann, A. Abbadie, A.M. Papon, P. Holliger, G. Rolland, T. Billon, J.M. Fédéli, M. Rouvière, L. Vivien, S. Laval, J. Appl. Phys. 95 (2004) 5905.
[13] J.-M. Hartmann, A.M. Papon, V. Destefanis, T. Billon, J. Cryst. Growth 310 (2008) 5287.
[14] R. Soref, J. Kouvetakis, J. Menendez, Mater. Res. Soc. Symp. Proc. 958 (2007) 13.
[15] M. El Kurdi, G. Fishman, S. Sauvage, P. Boucaud, J. Appl. Phys. 107 (2010) 013710.
[16] X. Sun, J.F. Liu, L.C. Kimerling, J. Michel, Appl. Phys. Lett. 95 (2009) 011911.
[17] M. El Kurdi, T. Kociniewski, T.-P. Ngo, J. Boulmer, D. Débarre, P. Boucaud, J.F. Damlencourt, O. Kermarrec, D. Bensahel, Appl. Phys. Lett. 94 (2009) 191107.
[18] V. Le Thanh, Surf. Sci. 492 (2001) 255(and references therein).
[19] L. Colace, G. Masini, F. Galluzzi, G. Assanto, G. Capellini, L. Di Gaspare, E. Pelange, F. Evangelisti, Appl. Phys. Lett. 72 (1998) 3175.
[20] H.-C. Luan, D.R. Lim, K.K. Lee, K.M. Chen, J.G. Sandland, K. Wada, L.C. Kimerling, Appl. Phys. Lett. 75 (1999) 2909.
[21] M. Halbwax, D. Bouchier, V. Yam, D. Débarre, Lam H. Nguyen, Y. Zheng, P. Rosner, M. Benamara, H.P. Strunk, C. Clerc, J. Appl. Phys. 97 (2005) 064907.
[22] V. Le Thanh, D. Bouchier, G. Hincelin, J. Appl. Phys. 87 (2000) 3700.
[23] T.K.P. Luong, M.T. Dau, M.A. Zrir, M. Stoffel, V. Le Thanh, M. Petit, A. Ghrib, M. El Kurdi, P. Boucaud, H. Rinnert, J. Murota, J. Appl. Phys. 114 (2013) 083504.
[24] H.J. McSkimin, P. Andreatch Jr., J. Appl. Phys. 34 (1963) 651.
[25] G. Lippert, H.J. Osten, D. Krüger, P. Gaworzewski, K. Eberl, Appl. Phys. Lett. 66 (1995) 3197.
[26] R.W. Olesinski, N. Kanani, G.J. Abbaschian, Bull. Alloy Phase Diagr. 6 (1985) 130.
[27] M. Oehme, J. Werner, E. Kasper, J. Cryst. Growth 310 (2008) 4531.